



**HAL**  
open science

## **De novo TUBB2B mutation causes fetal akinesia deformation sequence with microlissencephaly: an unusual presentation of tubulinopathy**

Annie Laquerrière, Marie Gonzales, Yoann Saillour, Mara Cavallin, Nicole Joyē, Chloé Quēlin, Laurent Bidat, Marc Dommergues, Ghislaine Plessis, Ferechte Encha-Razavi, et al.

### ► To cite this version:

Annie Laquerrière, Marie Gonzales, Yoann Saillour, Mara Cavallin, Nicole Joyē, et al.. De novo TUBB2B mutation causes fetal akinesia deformation sequence with microlissencephaly: an unusual presentation of tubulinopathy. *European Journal of Medical Genetics*, 2015, 59 (4), pp.249-256. 10.1016/j.ejmg.2015.12.007 . hal-01259440

**HAL Id: hal-01259440**

**<https://univ-rennes.hal.science/hal-01259440>**

Submitted on 6 Jun 2016

**HAL** is a multi-disciplinary open access archive for the deposit and dissemination of scientific research documents, whether they are published or not. The documents may come from teaching and research institutions in France or abroad, or from public or private research centers.

L'archive ouverte pluridisciplinaire **HAL**, est destinée au dépôt et à la diffusion de documents scientifiques de niveau recherche, publiés ou non, émanant des établissements d'enseignement et de recherche français ou étrangers, des laboratoires publics ou privés.

1 ***De novo TUBB2B* mutation causes fetal akinesia deformation sequence with**  
2 **microlissencephaly: an unusual presentation of tubulinopathy**

3 **Running Title:** Fetal akinesia sequence due to *TUBB2B* mutations

4  
5 Annie LAQUERRIERE (1,2), Marie GONZALES (3,4), Yoann SAILLOUR (5-7), Mara  
6 CAVALLIN (7-9), Nicole JOYÈ (3,4), Chloé QUÉLIN (10), Laurent BIDAT (11), Marc  
7 DOMMERGUES (4,12), Ghislaine PLESSIS (13), Ferechte ENCHA-RAZAVI (7,8,14),  
8 Jamel CHELLY (15,16), Nadia BAHI-BUISSON (7-9)\*, Karine POIRIER(5-7)\*

9 \* Both authors contributed equally to the manuscript

10

#### 11 **AFFILIATIONS:**

12 1 - Pathology Laboratory, Rouen University Hospital, France

13 2- Region-Inserm Team NeoVasc ERI28, Laboratory of Microvascular Endothelium and  
14 Neonate Brain Lesions, Institute of Research Innovation in Biomedicine, Normandy  
15 University, Rouen, France

16 3 - Department of Medical Genetics, Armand Trousseau Hospital, APHP, Paris, France

17 4 - Sorbonne Universities, UPMC, Paris, France

18 5 - Inserm, U1016, Institut Cochin, Paris, France

19 6- CNRS, UMR8104, Paris, France

20 7 - Paris Descartes - Sorbonne Paris Cité University, Imagine Institute, Paris, France

21 8-Pediatric Neurology, Necker Enfants Malades University Hospital, Paris, France

22 9- INSERM UMR-1163, Embryology and genetics of congenital malformation Université

23 Paris Descartes-Sorbonne Paris Cité, Institut Imagine, Université Paris Descartes-Sorbonne  
24 Paris Cité, France

25 10-Department of Clinical Genetics, South University Hospital, Rennes, France

26 11 - Department of Prenatal Diagnosis, Department of Obstetrics and Gynecology, René Dubos Hospital,  
27 Pontoise, France

28 12 - Department of Obstetrics and Gynecology, Groupe Hospitalier Pitié Salpêtrière, APHP,  
29 Paris, France

30 13 - Department of Genetics, Clinical Genetics, Caen University Hospital, Caen, France

31 14 - Département de Génétique, Necker-Enfants Malades University Hospital, Paris, France  
15 - Pôle de biologie, Hôpitaux Universitaires de Strasbourg, Strasbourg, France  
32 16 - Institut de Génétique et Biologie Moléculaire et Cellulaire - IGBMC, INSERM, CNRS,  
33 Université de Strasbourg, Strasbourg, France

34

35

36 **Corresponding author's information**

37 ***Nadia Bahi-Buisson, MD, PhD***

38 Université Paris Descartes-Sorbonne Paris Cité, Institut Imagine-INSERM UMR-1163,  
39 Embryology and genetics of congenital malformations

40 Email: [nadia.bahi-buisson@nck.aphp.fr](mailto:nadia.bahi-buisson@nck.aphp.fr)

41 Phone +33 1 42192699

42 Fax +33 1 42192692

43

44 **Clinical Report**

45 Word Count for the abstract 166

46 Word Count for the text 2515

47 Character count for the title 16

48 Number of figures 5

49 Supplementary figures : 2

50 References 26

51

52 **ABSTRACT**

53 Tubulinopathies are increasingly emerging major causes underlying complex cerebral  
54 malformations, particularly in case of microlissencephaly often associated with hypoplastic or  
55 absent corticospinal tracts. Fetal akinesia deformation sequence (FADS) refers to a clinically  
56 and genetically heterogeneous group of disorders with congenital malformations related to  
57 impaired fetal movement.

58 We report on an early foetal case with FADS and microlissencephaly due to *TUBB2B*  
59 mutation. Neuropathological examination disclosed virtually absent cortical lamination, foci  
60 of neuronal overmigration into the leptomeningeal spaces, corpus callosum agenesis,  
61 cerebellar and brainstem hypoplasia and extremely severe hypoplasia of the spinal cord with  
62 no anterior and posterior horns and almost no motoneurons.

63 At the cellular level, the p.Cys239Phe *TUBB2B* mutant leads to tubulin heterodimerization  
64 impairment, decreased ability to incorporate into the cytoskeleton, microtubule dynamics  
65 alteration, with an accelerated rate of depolymerization.

66 To our knowledge, this is the first case of microlissencephaly to be reported presenting with a  
67 so severe and early form of FADS, highlighting the importance of tubulin mutation screening  
68 in the context of FADS with microlissencephaly.

69

70

71

72 **KEY WORDS**

73 microlissencephaly, microcephaly, migration disorder, *TUBB2B*, Fetal akinesia deformation  
74 sequence

## 75 INTRODUCTION

76 Normal fetal development is dependent on adequate fetal movement, starting at 8 weeks of  
77 gestation (WG). Limitation of movements results in fetal akinesia deformation sequence  
78 (FADS; OMIM 208150). FADS was first reported as a syndrome by Pena and Shokeir in  
79 1974 and further delineated as a symptom by Hall in 1981 [1,2]. Its incidence varies among  
80 different countries and has been estimated at 1:3000 to 1:5000 by Fahy and Hall [3]. The  
81 clinical presentation is highly variable, ranging from the most severe form called lethal  
82 multiple pterygium syndrome characterized by multiple joint contractures and pterygia, lung  
83 hypoplasia, short umbilical cord, craniofacial changes consisting of hypertelorism,  
84 micrognathism, cleft palate, short neck, low-set ears, along with intrauterine growth  
85 retardation and abnormal amniotic fluid volume mainly observed from the first trimester of  
86 the pregnancy [4]. Less severe phenotypes may present either as distal arthrogryposis or as  
87 fetal hypomotility which usually occurs during the third trimester [5].

88 Non-genetic factors may cause FADS, such as environmental limitation of fetal movements,  
89 maternal infection, drugs and immune mechanisms (maternal autoimmune myasthenia). The  
90 FADS phenotype is observed in a number of known genetic syndromes. Non syndromic or  
91 isolated FADS is genetically heterogeneous and encompass multiple neurogenic processes  
92 affecting the central or the peripheral nervous system, the neuromuscular junction and the  
93 skeletal muscle [6-8]. Until recently, the neurogenic form characterized by spinal cord  
94 motoneuron paucity, either isolated or associated with pontocerebellar hypoplasia was  
95 considered as the most frequent cause [9-11]. Conversely, brain malformations are very  
96 infrequently observed in association with FADS, and mainly described in lissencephalies type  
97 I and II as deformations of the extremities [12,13]. To our knowledge, FADS has never been  
98 reported in association with tubulin related cortical malformations. Here, we report on the  
99 most severe presentation of tubulinopathy in a fetus harboring a *de novo* missense mutation in

100 the  $\beta$ -tubulin gene *TUBB2B* gene (MIM 615101), along with neuropathology and molecular  
101 data focusing on the consequences of the mutation, that could explain at least partly the  
102 severity of the lesions and early fetal presentation.

### 103 **PATIENT AND METHODS**

#### 104 **Case history**

105 A 32-year-old woman, gravida 4, para 3, underwent routine ultrasonography (US) at 12 WG,  
106 which revealed severe fetal akinesia. Control ultrasound examination performed at 14 WG  
107 confirmed total lack of movements, retrognathia and dilatation of the third and fourth cerebral  
108 ventricles (supplementary figure 1). A medical termination of the pregnancy was achieved at  
109 15 WG, in accordance with French law. A complete autopsy was performed with informed  
110 written consent from both parents. Brain lesions identified at autopsy suggested a possible  
111 Walker Warburg syndrome (WWS) despite absent eye lesions, so that a first-line screening of  
112 WWS genes was performed, but was negative. Indeed, known environmental causes of FADS  
113 were excluded, as well as syndromic causes. Chromosomal analysis performed on trophoblast  
114 biopsy revealed a normal male karyotype, 46, XY. The parents were non consanguinous and  
115 there was no relevant personal or family history. Three children born to a previous marriage  
116 were in good health.

117 After having obtained written informed consent from the parents, DNAs were purified from  
118 fetal lung tissues, and from peripheral blood cells in both parents by using a standard  
119 phenol/chloroform method. Mutation analysis was performed by PCR amplification and  
120 direct SANGER sequencing of all coding exons and splice sites of the *TUBB2B* gene revealed  
121 a *de novo* missense mutation in exon 4, c.716G>T determining a p.Cys239Phe substitution  
122 (previously reported in [14]). No other variant was identified after sequencing of the other  
123 genes involved in cortical malformations.

#### 124 **Neuropathological evaluation**

125 Tissues including the brain, eyes and spinal cord were fixed in a 10% formalin-zinc buffer  
126 solution. Seven-micrometer sections obtained from paraffin-embedded tissues were stained  
127 using Haematoxylin-Eosin. Adjacent brain and spinal cord sections were assessed for routine  
128 immunohistochemistry, using antibodies directed against vimentin (diluted 1:100; Dakopatts,  
129 Trappes, France), calretinin (1:200; Zymed Clinisciences, Montrouge, France), and MAP2  
130 (diluted 1:50, Sigma, St Louis, MO). Immunohistochemical procedures included a microwave  
131 pre-treatment protocol to aid antigen retrieval (pretreatment CC1 kit, Ventana Medical  
132 Systems Inc, Tucson AZ). Incubations were performed for 32 minutes at room temperature  
133 using the Ventana Benchmark XT system. After incubation, slides were processed by the  
134 Ultraview Universal DAB detection kit (Ventana). All immunolabellings were compared with  
135 an age matched control case examined after a spontaneous abortion for premature rupture of  
136 the membranes, and whose brain was histologically normal.

### 137 **Functional analyses**

#### 138 *Protein modeling*

139 A model of human  $\beta$ -tubulin was built by homology modeling using available structures  
140 (Research Collaboratory for Structural Bioinformatics PDB code 1TUB) from Nogales et al.  
141 [15]. The images in Figure 4C were rendered using PyMOL software  
142 (<http://www.pymol.org>).

#### 143 *Cloning and in vitro translation*

144 *TUBB2B* sequence was generated by PCR using a template from the human brain cDNA  
145 library (Clontech, Mountain View, CA). The PCR product was cloned into the pcDNA 3.1-  
146 V5-His vector (Invitrogen, Carlsbad, CA) and checked by DNA sequencing. These products  
147 were cloned both into the cDNA3.1-V5-his-TOPO-TA cloning vector (Invitrogen) and pET  
148 vector. An in-frame tag encoding the FLAG epitope (DYKDDDDK) was incorporated by  
149 PCR along with the C-terminus of the *TUBB2B* wild-type sequence allowing for the

150 distinction of the transgene from other highly homologous endogenously expressed  $\beta$ -tubulin  
151 polypeptides. The p.Cys239Phe mutation was introduced by site-directed mutagenesis using a  
152 QuikChange II kit (Stratagene, La Jolla, CA) and verified by DNA sequencing.  
153 Transcription/translation reactions were performed at 30°C for 90 min in 25  $\mu$ l of rabbit  
154 reticulocyte lysate (TNT; Promega, Madison, WI) containing  $^{35}$ S-methionine (specific  
155 activity, 1000 Ci/ $\mu$ mol; 10  $\mu$ Ci/ $\mu$ l). For the generation of labelled  $\beta$ -tubulin heterodimers,  
156 transcription/translation reactions were chased for a further 2 h at 30°C by the addition of  
157 0.375 mg/ml of native bovine brain tubulin. Aliquots (2  $\mu$ l) were withdrawn from the  
158 reaction, diluted into 10  $\mu$ l of gel-loading buffer (gel running buffer supplemented with 10%  
159 glycerol and 0.1% bromophenol blue) and stored on ice prior to resolution on a non-  
160 denaturing gel. Labeled reaction products were detected by autoradiography after resolution  
161 on either SDS-PAGE or on native polyacrylamide gels as described [16,17].

#### 162 *Cell cultures, transfections and immunofluorescence*

163 Primary cultures of fibroblasts were derived from fibroblastic cells extracted from amniotic  
164 liquid. COS7 and Hela cells were transfected by construct with p.Cys239Phe TUBB2B  
165 mutation using the Fugene 6 transfection reagent (Roche Applied Science, Indianapolis, IN)  
166 and grown on glass cover slips in Dulbecco's modified Eagle's medium containing 10% fetal  
167 calf serum and antibiotics. The cells were fixed with ice-cold methanol, 24–48h after growth.  
168 In the depolymerization experiments used to determine the behavioural stability of  
169 microtubules after 24 h of culture, fibroblasts were incubated for various brief intervals from  
170 0 to 30 min on ice and fixed thereafter. Repolymerization experiments were performed by  
171 successively exposing cells at 4°C during 30mn and fixed after being incubated from 0 to 15  
172 min at 37°C. Cells were then labelled with a polyclonal anti-FLAG antibody (1/500), or a  
173 monoclonal anti- $\alpha$ -tubulin antibody (1/1000) (Sigma-Aldrich Inc., St Louis, MO). At each  
174 experimental point, two parameters were quantified using ImageJ software: (i) the total area

175 of the cell and (ii) the area of the microtubules network of each cell, evaluated by  
176 quantifying the alpha-tubulin staining into the cytoskeleton and excluding the staining  
177 background corresponding to unincorporated alpha tubulin into the cellular cytoplasm. The  
178 ratio Microtubules Area/Total cell Area was used to evaluate the state of the microtubule  
179 network of the patient and control cells at each time point of  
180 depolymerisation/repolymerization experiments.

181

182

## 183 **RESULTS**

### 184 **General autopsy findings**

185 The fetus weighed 47g (50<sup>th</sup> centile). External examination disclosed cranio-facial  
186 dysmorphism with microretrognathia and cleft palate due to akinesia (supplementary figure  
187 2), global amyotrophy and microcephaly (Figure 1A). No internal visceral malformation was  
188 found, except for the lungs which were hypoplastic, and the renal pelvis which was dilated.

### 189 **Neuropathological studies**

190 Macroscopically, the brain appeared to be small, weighting 2.15g (5<sup>th</sup> centile, normal weight  
191 = 10g according to Guilhard-Costa and Larroche [18]). Occipito-frontal length was 21mm and  
192 transverse diameter of the cerebellum was 0.17 mm (25<sup>th</sup> centile). The brain surface was  
193 smooth, covered by thickened leptomeninges adherent to the brain (Figure 1B). Olfactory  
194 tracts were absent and the meninges seemed fused (Figure 1C). On brainstem sections, the  
195 fourth ventricle was dilated and the cerebellum seemed hypoplastic and dysplastic,  
196 resembling the cerebellar dysplasia observed in Walker Warburg syndrome (Figure 1D).  
197 Macroscopic examination of serial coronal sections confirmed the dilatation of the third and  
198 lateral ventricles, the latter being filled with congestive choroid plexuses.

199 Histological examination of the eyes revealed no retinal dysplasia. The spinal cord displayed  
200 major lesions consisting of severe hypoplasia and immaturity (Figure 2A). Ascending and  
201 descending tracts were missing. Anterior and posterior horns were hardly discernible, with  
202 almost no motoneurons in the anterior horns, even using MAP2 antibodies (data not shown)  
203 (Figure 2B). The cerebral mantle was particularly thin, and cortical lamination was absent,  
204 rather forming an extremely disorganized two-layered cortex extending from the inferior limit  
205 of the marginal zone to the periventricular zone with no recognizable intermediate zone  
206 (Figure 2C). Layer I was irregular in width and contained isolated or small foci of immature  
207 neurons, as well as misplaced Cajal-Retzius cells immunolabeled by calretinin antibody lying  
208 under the pial basal membrane (Figure 2D). Underneath, a single band of neurons with a  
209 vague nodular or columnar organization was found, extending to the periventricular areas  
210 (Figure 2E). The cerebral mantle was covered by fibrous meninges containing multiple  
211 dysplastic tortuous vessels with dispersed overmigrating immature neurons (Figure 2F).  
212 Vimentin immunohistochemistry showed an irregular and fragmented glia limitans (Figure  
213 3A and B), with small gaps through which neurons overmigrated into the leptomeningeal  
214 spaces (Figure 3C, D). Vimentin immunohistochemistry also revealed severe abnormalities of  
215 the radial glia, which virtually absent in the cortical plate and entirely disorganized in the  
216 subventricular zone (Figure 3E and F).

## 217 **Functional analyses**

### 218 *Consequences of the mutation on secondary and tertiary TUBB2B structures*

219 The p.Cys239 residue is located in the intermediary domain (amino acid 205–381) of the  
220 TUBB2B protein and is highly conserved during evolution among TUBB2B homologues  
221 from other species (Figure 4A). Tridimensional modeling analysis of TUBB2B using PYmol  
222 software displayed an inside localization of the variant in an helix closed to the Taxol fixation

223 site, apparently affecting neither the GDP binding pocket nor the  $\alpha/\beta$  interacting region  
224 (Figure 4B).

225 *Alteration of  $\alpha/\beta$  heterodimerization process and microtubules incorporation by TUBB2B*  
226 *variant*

227 To further investigate functional consequences of the mutation, the  $\beta$ -tubulin mutant was  
228 expressed in rabbit reticulocyte lysate and its ability to assemble into  $\alpha/\beta$  heterodimers in the  
229 presence of bovine brain tubulin was evaluated. The p.Cys239Phe mutant was translated as  
230 efficiently as the wild-type control (Figure 5A). However, analysis of the same reaction  
231 products under native conditions revealed a range of heterodimer formation that was  
232 significantly decreased both quantitatively and qualitatively in the case of p.Cys239Phe  
233 mutant compared to the wild-type control (Figure 5B) revealing an impairment of tubulin  
234 heterodimerization processes in the p.Cys239Phe mutant.

235 Furthermore, the transfection of the flag-tagged p.Cys239Phe *TUBB2B*-mutated construct in  
236 COS7 and HeLa cells revealed both a detectable incorporation of the protein into  
237 microtubules and in contrast to controls, a diffuse high background of label that reflects  
238 presence of unpolymerized cytosolic tubulin heterodimers, suggesting a partial impairment of  
239 the remaining heterodimer ability to incorporate into the cytoskeleton (Figure 5C).

240 *Effects of p.Cys239Phe TUBB2B mutation on the dynamical microtubule behavior in fetal*  
241 *fibroblasts*

242 In order to assess the behavior of the microtubules *in vivo*, we analyzed the response of the  
243 cytoskeleton to cold-induced depolymerization treatment followed by a repolymerization step  
244 at 37°C in fibroblasts extracted from amniotic liquid from control and affected patient.

245 Following cold-induced depolymerization, *TUBB2B* p.Cys239Phe displayed a normal rate of  
246 microtubules disintegration (Figure 5C). However, repolymerization experiments, consisting  
247 in a completed cytoskeleton depolymerization at 4°C and a gradual repolymerisation at 37°C,

248 revealed that p.Cys239Phe *TUBB2B* mutant microtubules are more repolymerized after  
249 5min at 37°C than controls (Figure 5C). These experiments show that with p.Cys239Phe  
250 mutant, the repolymerization rate to renew its cytoskeleton network is accelerated, provoking  
251 a defect of the depolymerization/repolymerization balance necessary for a proper dynamic  
252 behaviour of microtubules.

## 253 **DISCUSSION**

254 We report here the first case of Fetal Akinesia Deformation Sequence with  
255 microlissencephaly related to *TUBB2B* mutation, expanding the phenotype of ever-growing  
256 family of *tubulin* associated malformations. The diagnosis of FADS can be approached  
257 algorithmically, based on the presence of neurological symptoms and associated features  
258 [19,6]. Developmental abnormalities affecting the forebrain (e.g., hydranencephaly,  
259 microcephaly, or forebrain neuronal migration disorders), either due to primary genetic  
260 factors or to a consequence of fetal central nervous system infection or vascular insult, are  
261 sometimes associated with arthrogryposis [6,20]. In such cases, joint contractures are thought  
262 to be related to diminished corticospinal tract activation of spinal cord motor neurons.  
263 Sometimes, however, the underlying disease also directly affects spinal cord motor neurons,  
264 contributing to fetal akinesia or hypomotility. In addition to these classical causes, our report  
265 demonstrates that tubulin related microlissencephaly should be considered within the  
266 algorithm for diagnosis.

267 Microlissencephaly is a rare entity characterized by severe congenital microcephaly with  
268 absent sulci and gyri leading most of the time to an early fatal outcome during the foetal or  
269 the neonatal period. We have previously underlined the importance of microlissencephaly in  
270 the spectrum of tubulinopathies [14]. There are emerging molecular data to suggest that  
271 *NDE1* mutations [21,22] and more recently *KATNB1* mutations [23] are involved in the  
272 autosomal recessive forms. Tubulin mutations, particularly *TUBA1A* and less frequently

273 *TUBB2B* and *TUBB3* are significant causes of sporadic cases of microlissencephaly.  
274 Tubulin related microlissencephaly share common features consisting in corpus callosum  
275 agenesis, extremely reduced or absent cortical plate, hypertrophic germinal zones and  
276 ganglionic eminences, hypoplastic and disorganized striatum and thalami. In our case, the  
277 striatum and thalami were absent, along with germinative zones in which radial glial cells and  
278 radial glia had early disappeared, representing the most severe end of the spectrum. At the  
279 infratentorial level, our case also showed common signs of tubulin related  
280 microlissencephaly, i.e. severe cerebellar and brainstem hypoplasia, axon tract defects with  
281 absent corticospinal tracts. To our knowledge, 13 foetal cases with tubulin related  
282 microlissencephaly [14,24] and 4 living patients [24,25] have been reported so far. Of these, 8  
283 exhibited non specific dysmorphic features including retrognathia and hypertelorism, as well  
284 as adducted thumbs, extremely long fingers, and rocker bottom feet related to poor fetal  
285 mobility. The case reported here represents the extreme severe end of the spectrum due to  
286 extremely severe spinal cord hypoplasia with absent anterior and posterior horns and virtually  
287 indiscernible motoneurons at the histological level. In this context, fetal akinesia deformation  
288 sequence undoubtedly represents a neurogenic form, reminiscent of akinesia observed in  
289 Spinal Muscular Atrophy or fetal Pontocerebellar Hypoplasia type 1 [9-11].  
290 The precise molecular function of *TUBB2B* in cortical development still remains unclear. Our  
291 analysis suggests that the aminoacid substitution in the p.Cys239Phe *TUBB2B* mutant leads  
292 to an impairment of tubulin heterodimerization processes and heterodimer ability to  
293 incorporate into the cytoskeleton. Moreover, this mutant alters the microtubule dynamics with  
294 an accelerated rate of repolymerization, that is has been also predicted with another *TUBB2B*  
295 related microlissencephaly mutation (p.Asp249His) [26]. In the literature, we already  
296 demonstrated that two *TUBA1A* and *TUBB2B* mutants' cells (p.Pro263Thr and p.Ser172Pro,  
297 respectively) display an opposite phenotype consisting of a defect to renew their cytoskeleton

298 network after total depolymerization, we assume that the two types of repolymerization  
299 impairments lead to abnormalities of the depolymerization/repolymerization balance  
300 necessary for a proper dynamic behaviour of microtubules [27 ,28]. As suggesting in the  
301 literature, a default in microtubules dynamics could lead to dramatic impairments of a  
302 numerous cellular processes including proliferation, migration and differentiation that are  
303 crucial steps for the brain development [28 ,29 ,30]. Therefore, we assume that this alteration  
304 of microtubule dynamics might affect brain and spinal cord development at distinct  
305 developmental steps, i.e. neurogenesis, neuronal migration and long tract formation, leading  
306 to the association of FADS and microlissencephaly. According to structural molecular  
307 models, the mutant p.Cys239Phe is predicted to alter tubulin folding. This extreme phenotype  
308 contrasts with our previous observations in which tubulin mutations predicted to impair  
309 tubulin folding but tended to be associated with milder cortical malformations [26] and  
310 emphasizes on the fact that comprehensive overview of tubulinopathies spectrum will require  
311 further investigations, including understanding of spatial and temporal consequences of  
312 tubulin mutations on MT-dependent cellular functions and early neuro-developmental  
313 processes.

314 In conclusion, this fetal case recapitulates the phenotypic features of tubulin related  
315 microlissencephaly expands the phenotype due to early severe arthrogryposis and underlines  
316 the importance of considering tubulin gene *TUBB2B* in the diagnosis of arthrogryposis with  
317 microlissencephaly.

#### 318 **ACKNOWLEDGMENTS**

319 We would like to thank Prof. Beldjord for their careful reading and constructive comments,  
320 Dr Lascelles for her advice on improving the manuscript, and Dr Sandrine Vuillaumier-Barrot  
321 and Odile Philippon. The research leading to these results was funded by the European Union

322 Seventh Framework Programme FP7/2007-2013 under the project DESIRE (grant  
323 agreement n°602531). KP, NBB and JC were supported in part by a « Rare Diseases  
324 Foundation » grant.

## 325 REFERENCES

- 326 1. Hall JG (1981) An approach to congenital contractures (arthrogryposis). *Pediatric annals* 10  
327 (7):15-26
- 328 2. Haliloglu G, Topaloglu H (2013) Arthrogryposis and fetal hypomobility syndrome.  
329 *Handbook of clinical neurology* 113:1311-1319. doi:10.1016/B978-0-444-59565-2.00003-4
- 330 3. Fahy MJ, Hall JG (1990) A retrospective study of pregnancy complications among 828  
331 cases of arthrogryposis. *Genetic counseling* 1 (1):3-11
- 332 4. Hammond E, Donnfeld AE (1995) Fetal akinesia. *Obstetrical & gynecological survey* 50  
333 (3):240-249
- 334 5. Pena SD, Shokeir MH (1974) Autosomal recessive cerebro-oculo-facio-skeletal (COFS)  
335 syndrome. *Clin Genet* 5 (4):285-293
- 336 6. Bamshad M, Van Heest AE, Pleasure D (2009) Arthrogryposis: a review and update. *The*  
337 *Journal of bone and joint surgery American volume* 91 Suppl 4:40-46.  
338 doi:10.2106/JBJS.I.00281
- 339 7. Navti OB, Kinning E, Vasudevan P, Barrow M, Porter H, Howarth E, Konje J, Khare M  
340 (2010) Review of perinatal management of arthrogryposis at a large UK teaching hospital  
341 serving a multiethnic population. *Prenatal diagnosis* 30 (1):49-56. doi:10.1002/pd.2411
- 342 8. Laquerriere A, Maluenda J, Camus A, Fontenas L, Dieterich K, Nolent F, Zhou J, Monnier  
343 N, Latour P, Gentil D, Heron D, Desguerres I, Landrieu P, Beneteau C, Delaporte B,  
344 Bellesme C, Baumann C, Capri Y, Goldenberg A, Lyonnet S, Bonneau D, Estournet B,  
345 Quijano-Roy S, Francannet C, Odent S, Saint-Frison MH, Sigaudy S, Figarella-Branger D,  
346 Gelot A, Mussini JM, Lacroix C, Drouin-Garraud V, Malinge MC, Attie-Bitach T, Bessieres  
347 B, Bonniere M, Encha-Razavi F, Beaufriere AM, Khung-Savatovsky S, Perez MJ, Vasiljevic  
348 A, Mercier S, Roume J, Trestard L, Saugier-veber P, Cordier MP, Layet V, Legendre M,  
349 Vigouroux-Castera A, Lunardi J, Bayes M, Jouk PS, Rigonnot L, Granier M, Sternberg D,  
350 Warszawski J, Gut I, Gonzales M, Tawk M, Melki J (2014) Mutations in CNTNAP1 and  
351 ADCY6 are responsible for severe arthrogryposis multiplex congenita with axoglial defects.  
352 *Human molecular genetics* 23 (9):2279-2289. doi:10.1093/hmg/ddt618
- 353 9. Banker BQ (1986) Arthrogryposis multiplex congenita: spectrum of pathologic changes.  
354 *Human pathology* 17 (7):656-672
- 355 10. Vuopala K, Ignatius J, Herva R (1995) Lethal arthrogryposis with anterior horn cell  
356 disease. *Human pathology* 26 (1):12-19
- 357 11. Vuopala K, Makela-Bengs P, Suomalainen A, Herva R, Leisti J, Peltonen L (1995) Lethal  
358 congenital contracture syndrome (LCCS), a fetal anterior horn cell disease, is not linked to the  
359 SMA 5q locus. *J Med Genet* 32 (1):36-38
- 360 12. Devisme L, Bouchet C, Gonzales M, Alanio E, Bazin A, Bessieres B, Bigi N, Blanchet P,  
361 Bonneau D, Bonnières M, Bucourt M, Carles D, Clarisse B, Delahaye S, Fallet-Bianco C,  
362 Figarella-Branger D, Gaillard D, Gasser B, Delezoide AL, Guimiot F, Joubert M, Laurent N,

- 363 Laquerriere A, Liprandi A, Loget P, Marcorelles P, Martinovic J, Menez F, Patrier S,  
364 Pelluard F, Perez MJ, Rouleau C, Triaux S, Attie-Bitach T, Vuillaumier-Barrot S, Seta N,  
365 Encha-Razavi F (2012) Cobblestone lissencephaly: neuropathological subtypes and  
366 correlations with genes of dystroglycanopathies. *Brain* 135 (Pt 2):469-482.  
367 doi:10.1093/brain/awr357
- 368 13. Witters I, Moerman P, Fryns JP (2002) Fetal akinesia deformation sequence: a study of 30  
369 consecutive in utero diagnoses. *American journal of medical genetics* 113 (1):23-28.  
370 doi:10.1002/ajmg.10698
- 371 14. Fallet-Bianco C, Laquerriere A, Poirier K, Razavi F, Guimiot F, Dias P, Loeuillet L,  
372 Lascelles K, Beldjord C, Carion N, Toussaint A, Revencu N, Addor MC, Lhermitte B,  
373 Gonzales M, Martinovich J, Bessieres B, Marcy-Bonniere M, Jossic F, Marcorelles P, Loget  
374 P, Chelly J, Bahi-Buisson N (2014) Mutations in tubulin genes are frequent causes of various  
375 foetal malformations of cortical development including microlissencephaly. *Acta*  
376 *neuropathologica communications* 2:69. doi:10.1186/2051-5960-2-69
- 377 15. Nogales E, Wolf SG, Downing KH (1998) Structure of the alpha beta tubulin dimer by  
378 electron crystallography. *Nature* 391 (6663):199-203. doi:10.1038/34465
- 379 16. Tian G, Huang Y, Rommelaere H, Vandekerckhove J, Ampe C, Cowan NJ (1996)  
380 Pathway leading to correctly folded beta-tubulin. *Cell* 86 (2):287-296. doi:S0092-  
381 8674(00)80100-2 [pii]
- 382 17. Tian G, Lewis SA, Feierbach B, Stearns T, Rommelaere H, Ampe C, Cowan NJ (1997)  
383 Tubulin subunits exist in an activated conformational state generated and maintained by  
384 protein cofactors. *J Cell Biol* 138 (4):821-832
- 385 18. Guihard-Costa AM, Larroche JC, Droulle P, Narcy F (1995) Fetal Biometry. Growth  
386 charts for practical use in fetopathology and antenatal ultrasonography. *Introduction. Fetal*  
387 *diagnosis and therapy* 10 (4):211-278
- 388 19. Kalampokas E, Kalampokas T, Sofoudis C, Deligeoroglou E, Botsis D (2012) Diagnosing  
389 arthrogryposis multiplex congenita: a review. *ISRN obstetrics and gynecology* 2012:264918.  
390 doi:10.5402/2012/264918
- 391 20. Chen CP (2012) Prenatal diagnosis and genetic analysis of fetal akinesia deformation  
392 sequence and multiple pterygium syndrome associated with neuromuscular junction  
393 disorders: a review. *Taiwanese journal of obstetrics & gynecology* 51 (1):12-17.  
394 doi:10.1016/j.tjog.2012.01.004
- 395 21. Alkuraya FS, Cai X, Emery C, Mochida GH, Al-Dosari MS, Felie JM, Hill RS, Barry BJ,  
396 Partlow JN, Gascon GG, Kentab A, Jan M, Shaheen R, Feng Y, Walsh CA (2011) Human  
397 mutations in NDE1 cause extreme microcephaly with lissencephaly [corrected]. *Am J Hum*  
398 *Genet* 88 (5):536-547. doi:10.1016/j.ajhg.2011.04.003
- 399 22. Bakircioglu M, Carvalho OP, Khurshid M, Cox JJ, Tuysuz B, Barak T, Yilmaz S,  
400 Caglayan O, Dincer A, Nicholas AK, Quarrell O, Springell K, Karbani G, Malik S, Gannon  
401 C, Sheridan E, Crosier M, Lisgo SN, Lindsay S, Bilguvar K, Gergely F, Gunel M, Woods CG  
402 (2011) The essential role of centrosomal NDE1 in human cerebral cortex neurogenesis. *Am J*  
403 *Hum Genet* 88 (5):523-535. doi:10.1016/j.ajhg.2011.03.019
- 404 23. Hu WF, Pomp O, Ben-Omran T, Kodani A, Henke K, Mochida GH, Yu TW, Woodworth  
405 MB, Bonnard C, Raj GS, Tan TT, Hamamy H, Masri A, Shboul M, Al Saffar M, Partlow JN,  
406 Al-Dosari M, Alazami A, Alowain M, Alkuraya FS, Reiter JF, Harris MP, Reversade B,  
407 Walsh CA (2014) Katanin p80 regulates human cortical development by limiting centriole  
408 and cilia number. *Neuron* 84 (6):1240-1257. doi:10.1016/j.neuron.2014.12.017

- 409 24. Kumar RA, Pilz DT, Babatz TD, Cushion TD, Harvey K, Topf M, Yates L, Robb S,  
410 Uyanik G, Mancini GM, Rees MI, Harvey RJ, Dobyns WB (2010) TUBA1A mutations cause  
411 wide spectrum lissencephaly (smooth brain) and suggest that multiple neuronal migration  
412 pathways converge on alpha tubulins. *Human molecular genetics* 19 (14):2817-2827
- 413 25. Cushion TD, Dobyns WB, Mullins JG, Stoodley N, Chung SK, Fry AE, Hehr U, Gunny  
414 R, Aylsworth AS, Prabhakar P, Uyanik G, Rankin J, Rees MI, Pilz DT (2013) Overlapping  
415 cortical malformations and mutations in TUBB2B and TUBA1A. *Brain* 136 (Pt 2):536-548.  
416 doi:10.1093/brain/aws338
- 417 26. Bahi-Buisson N, Poirier K, Fourniol F, Saillour Y, Valence S, Lebrun N, Hully M, Bianco  
418 CF, Boddaert N, Elie C, Lascelles K, Souville I, Consortium LI-T, Beldjord C, Chelly J  
419 (2014) The wide spectrum of tubulinopathies: what are the key features for the diagnosis?  
420 *Brain* 137 (Pt 6):1676-1700. doi:10.1093/brain/awu082
- 421 27. Tian G, Jaglin XH, Keays DA, Francis F, Chelly J, Cowan NJ (2010) Disease-associated  
422 mutations in TUBA1A result in a spectrum of defects in the tubulin folding and heterodimer  
423 assembly pathway. *Human molecular genetics* 19 (18):3599-3613
- 424 28. Jaglin XH, Chelly J (2009) Tubulin-related cortical dysgeneses: microtubule dysfunction  
425 underlying neuronal migration defects. *Trends Genet* 25 (12):555-566
- 426 29. Poirier K, Saillour Y, Bahi-Buisson N, Jaglin XH, Fallet-Bianco C, Nabbout R,  
427 Castelnau-Ptakhine L, Roubertie A, Attie-Bitach T, Desguerre I, Genevieve D, Barnerias C,  
428 Keren B, Lebrun N, Boddaert N, Encha-Razavi F, Chelly J (2010) Mutations in the neuronal  
429 ss-tubulin subunit TUBB3 result in malformation of cortical development and neuronal  
430 migration defects. *Human molecular genetics* 19 (22):4462-4473. doi:10.1093/hmg/ddq377
- 431 30. Saillour Y, Broix L, Bruel-Jungerman E, Lebrun N, Muraca G, Rucci J, Poirier K,  
432 Belvindrah R, Francis F, Chelly J (2013) Beta tubulin isoforms are not interchangeable for  
433 rescuing impaired radial migration due to Tubb3 knockdown. *Human molecular genetics*.  
434 doi:10.1093/hmg/ddt538

435  
436

437

## 438 LEGENDS TO THE FIGURES

439

440 Figure 1: Macroscopical findings

- 441 A. Severe foetal akinesia sequence with multiple deformations, joint contractures and  
442 pterygia, along with severe global amyotrophy
- 443 B. Superior view of the brain exhibiting a cobblestone-like appearance with abnormal  
444 meningeal vessels

- 445 C. Inferior view of the brain displaying absent interhemispheric fissure due to fusion of the  
446 meninges, absent olfactory bulbs and tracts and severely hypoplastic cerebellum  
447 D. With absent foliation and almost indiscernible vermis and cerebellar hemispheres.

448

449 Figure 2: Main histological lesions

- 450 A. Severe hypoplasia of the spinal cord (arrow) (H& E stain, OMx25)  
451 B. With at higher magnification, absent descending (arrow) and ascending tracts (triangle)  
452 and no motoneurons in the anterior horns (H& E stain, OMx250)  
453 C. Global disorganization of the cerebral mantle with no recognizable cortical plate,  
454 intermediate and germinal zones (H& E stain, OMx25)  
455 D. Calretinin immunohistochemistry showing aberrant Cajal Retzius cell location, with focal  
456 accumulation of these cells along the persisting glia limitans instead of forming a continuous  
457 streak located at the upper third of the molecular layer (OMx100)  
458 E. Microscopic view of the cortical plate displaying thickened leptomeninges with tortuous  
459 vessels, only a minority of them properly penetrating into the brain parenchyma (arrow) (H&  
460 E stain, OMx100)  
461 F. Absent lamination of the cortical plate replaced by nodules or columns of neurons, some of  
462 them overmigrating into the leptomeningeal spaces (arrow) (H& E stain, OMx250)

463

464 Figure 3: Vimentin immunohistochemical studies

- 465 A. Irregular thickening of the meninges (OMx100)  
466 B. Compared with an age-matched control brain (OMx100)  
467 C. With immature neurons accumulating just under the fragmented glia limitans (arrow) and  
468 disorganized vascular network (OMx250)  
469 D. With abnormal fibrous walls (arrow) and absent radial glia (OMx400)

470 E. And paucity of radial glial cells( arrow) and fragmentation of the radial glia in the  
471 subventricular zone (OMx400)

472 F. Compared to an age-matched control brain where the neuroepithelium (arrow) and the  
473 subventricular zone are strongly immunolabeled (OMx400)

474 H&E: Haematoxylin and eosin, OM: original magnification

475

476 Figure 4: *TUBB2B* *de novo* missense mutation (p.Cys239Phe) responsible of the phenotype  
477 FADS with microlissencephaly.

478 A. Pedigree of the family and chromatograms showing the *de novo* occurrence of the  
479 *TUBB2B* p.Cys239Phe mutation. Square, male; round, female; diamond, fetus. Black colour,  
480 affected individual.

481 B. Evolution conservation of the p.Cys239 amino acid in orthologues from stickleback to  
482 human. C. Structural representation using Pymol software of the  $\alpha/\beta$  heterodimer depicted  
483 without (top left) or with (top right) surface delimitation. p.Cys239 amino acid (in green) is  
484 localized into an helix inside the monomer but outside GTP, GDP and taxol binding sites  
485 (detailed view, bottom). Pdb: 1TUB.

486

487 Figure 5: Defects in the  $\alpha/\beta$  heterodimerisation process in the microtubule incorporation and  
488 dynamical behaviour in COS7 and fibroblasts expressing the p.Cys239Phe mutation.

489 A. The p.Cys239Phe *TUBB2B* mutation results in inefficient  $\alpha/\beta$  heterodimer formation *in*  
490 *vitro*. Analysis by SDS-Page and non denaturing gel of *in vitro* translation products conducted  
491 with 35S methionine labeled wild type and p.Cys239Phe mutant. The reaction products were  
492 further chased with bovine brain tubulin to generate  $\alpha/\beta$  heterodimers. SDS-Page gel showed  
493 that the mutant was translated as efficiently as the wild type control. Note that in non  
494 denaturing gel condition, p.Cys239Phe mutant generated heterodimers in a diminished yield.

495 B. Expression of C-terminal Flag tagged *TUBB2B* wild type (left column) and  
496 p.Cys239Phe mutant (right column) in transfected COS7 cells revealed by antFLAG (top line)  
497 and  $\alpha$ -tubulin (bottom line) staining. Note that a part of p.Cys239Phe mutant proteins failed to  
498 incorporate into the microtubule network, producing a more diffuse cytosolic labeling pattern  
499 in comparison with WT *TUBB2B*.

500 C. *In vivo* analysis of cytoskeleton behaviour and stability using patient's fibroblasts from  
501 amniotic liquid. Evaluation of the sensitivity of microtubules to cold treatment and of its ability  
502 to repolymerize was analyzed in control fibroblasts and patient fibroblasts with p.Cys239Phe  
503 mutation after 8 min of cold treatment at 4°C (left graph) or after 20 min at 4°C and 5 min at  
504 37°C (right graph). Note that the fibroblasts of the fetus correctly reacted to cold treatment by  
505 showing an increase in capacity to repolymerize compared to the wild type control.

506  
507 **Supplementary figures**

508 Supplementary figure 1: US examination performed at 14 WG showing fetal (A) retrognathia  
509 and dilatation of the fourth cerebral ventricle (B)

510

511 Supplementary figure 2: Fetal examination displaying arthrogryposis with clenched hands  
512 (A), posterior cleft palate (B), antebrachial C) and axillary pterygia (D).

513

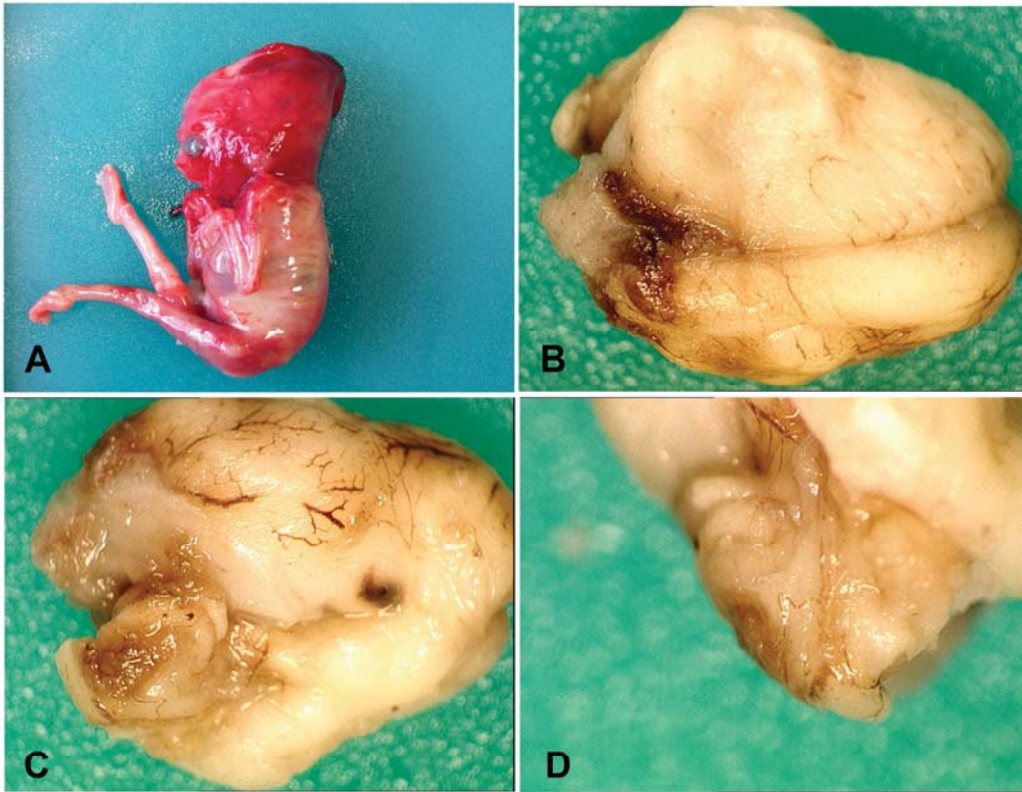
514

515

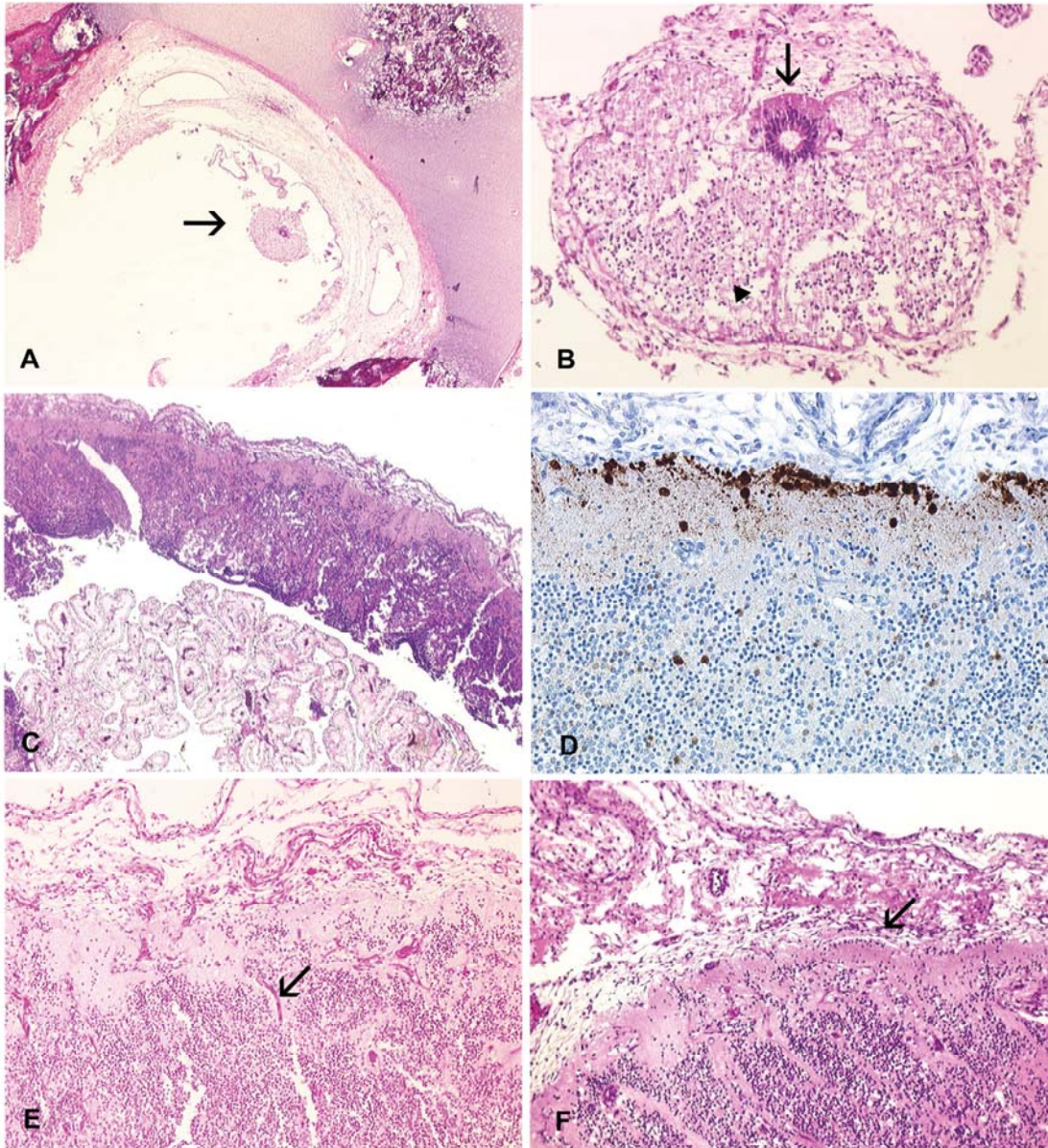
- 516 1. Hall JG (1981) An approach to congenital contractures (arthrogryposis). *Pediatric annals* 10  
517 (7):15-26
- 518 2. Haliloglu G, Topaloglu H (2013) Arthrogryposis and fetal hypomobility syndrome.  
519 *Handbook of clinical neurology* 113:1311-1319. doi:10.1016/B978-0-444-59565-2.00003-4
- 520 3. Fahy MJ, Hall JG (1990) A retrospective study of pregnancy complications among 828  
521 cases of arthrogryposis. *Genetic counseling* 1 (1):3-11
- 522 4. Hammond E, Donnenfeld AE (1995) Fetal akinesia. *Obstetrical & gynecological survey* 50  
523 (3):240-249
- 524 5. Pena SD, Shokeir MH (1974) Autosomal recessive cerebro-oculo-facio-skeletal (COFS)  
525 syndrome. *Clin Genet* 5 (4):285-293
- 526 6. Bamshad M, Van Heest AE, Pleasure D (2009) Arthrogryposis: a review and update. *The*  
527 *Journal of bone and joint surgery American volume* 91 Suppl 4:40-46.  
528 doi:10.2106/JBJS.I.00281
- 529 7. Navti OB, Kinning E, Vasudevan P, Barrow M, Porter H, Howarth E, Konje J, Khare M  
530 (2010) Review of perinatal management of arthrogryposis at a large UK teaching hospital  
531 serving a multiethnic population. *Prenatal diagnosis* 30 (1):49-56. doi:10.1002/pd.2411
- 532 8. Laquerriere A, Maluenda J, Camus A, Fontenas L, Dieterich K, Nolent F, Zhou J, Monnier  
533 N, Latour P, Gentil D, Heron D, Desguerres I, Landrieu P, Beneteau C, Delaporte B,  
534 Bellesme C, Baumann C, Capri Y, Goldenberg A, Lyonnet S, Bonneau D, Estournet B,  
535 Quijano-Roy S, Francannet C, Odent S, Saint-Frison MH, Sigaudy S, Figarella-Branger D,  
536 Gelot A, Mussini JM, Lacroix C, Drouin-Garraud V, Malinge MC, Attie-Bitach T, Bessieres  
537 B, Bonniere M, Encha-Razavi F, Beaufriere AM, Khung-Savatovsky S, Perez MJ, Vasiljevic  
538 A, Mercier S, Roume J, Trestard L, Saugier-Veber P, Cordier MP, Layet V, Legendre M,  
539 Vigouroux-Castera A, Lunardi J, Bayes M, Jouk PS, Rigonnot L, Granier M, Sternberg D,  
540 Warszawski J, Gut I, Gonzales M, Tawk M, Melki J (2014) Mutations in CNTNAP1 and  
541 ADCY6 are responsible for severe arthrogryposis multiplex congenita with axoglial defects.  
542 *Human molecular genetics* 23 (9):2279-2289. doi:10.1093/hmg/ddt618
- 543 9. Banker BQ (1986) Arthrogryposis multiplex congenita: spectrum of pathologic changes.  
544 *Human pathology* 17 (7):656-672
- 545 10. Vuopala K, Ignatius J, Herva R (1995) Lethal arthrogryposis with anterior horn cell  
546 disease. *Human pathology* 26 (1):12-19
- 547 11. Vuopala K, Makela-Bengts P, Suomalainen A, Herva R, Leisti J, Peltonen L (1995) Lethal  
548 congenital contracture syndrome (LCCS), a fetal anterior horn cell disease, is not linked to the  
549 SMA 5q locus. *J Med Genet* 32 (1):36-38
- 550 12. Devisme L, Bouchet C, Gonzales M, Alanio E, Bazin A, Bessieres B, Bigi N, Blanchet P,  
551 Bonneau D, Bonnieres M, Bucourt M, Carles D, Clarisse B, Delahaye S, Fallet-Bianco C,  
552 Figarella-Branger D, Gaillard D, Gasser B, Delezoide AL, Guimiot F, Joubert M, Laurent N,  
553 Laquerriere A, Liprandi A, Loget P, Marcorelles P, Martinovic J, Menez F, Patrier S, Pelluard  
554 F, Perez MJ, Rouleau C, Triau S, Attie-Bitach T, Vuillaumier-Barrot S, Seta N, Encha-Razavi  
555 F (2012) Cobblestone lissencephaly: neuropathological subtypes and correlations with genes  
556 of dystroglycanopathies. *Brain* 135 (Pt 2):469-482. doi:10.1093/brain/awr357
- 557 13. Witters I, Moerman P, Fryns JP (2002) Fetal akinesia deformation sequence: a study of 30  
558 consecutive in utero diagnoses. *American journal of medical genetics* 113 (1):23-28.  
559 doi:10.1002/ajmg.10698
- 560 14. Fallet-Bianco C, Laquerriere A, Poirier K, Razavi F, Guimiot F, Dias P, Loeuillet L,  
561 Lascelles K, Beldjord C, Carion N, Toussaint A, Revencu N, Addor MC, Lhermitte B,

- 562 Gonzales M, Martinovich J, Bessieres B, Marcy-Bonniere M, Jossic F, Marcorelles P,  
563 Loget P, Chelly J, Bahi-Buisson N (2014) Mutations in tubulin genes are frequent causes of  
564 various foetal malformations of cortical development including microlissencephaly. *Acta*  
565 *neuropathologica communications* 2:69. doi:10.1186/2051-5960-2-69
- 566 15. Nogales E, Wolf SG, Downing KH (1998) Structure of the alpha beta tubulin dimer by  
567 electron crystallography. *Nature* 391 (6663):199-203. doi:10.1038/34465
- 568 16. Tian G, Huang Y, Rommelaere H, Vandekerckhove J, Ampe C, Cowan NJ (1996)  
569 Pathway leading to correctly folded beta-tubulin. *Cell* 86 (2):287-296. doi:S0092-  
570 8674(00)80100-2 [pii]
- 571 17. Tian G, Lewis SA, Feierbach B, Stearns T, Rommelaere H, Ampe C, Cowan NJ (1997)  
572 Tubulin subunits exist in an activated conformational state generated and maintained by  
573 protein cofactors. *J Cell Biol* 138 (4):821-832
- 574 18. Guihard-Costa AM, Larroche JC, Droulle P, Narcy F (1995) Fetal Biometry. Growth  
575 charts for practical use in fetopathology and antenatal ultrasonography. *Introduction. Fetal*  
576 *diagnosis and therapy* 10 (4):211-278
- 577 19. Kalampokas E, Kalampokas T, Sofoudis C, Deligeoroglou E, Botsis D (2012) Diagnosing  
578 arthrogryposis multiplex congenita: a review. *ISRN obstetrics and gynecology* 2012:264918.  
579 doi:10.5402/2012/264918
- 580 20. Chen CP (2012) Prenatal diagnosis and genetic analysis of fetal akinesia deformation  
581 sequence and multiple pterygium syndrome associated with neuromuscular junction  
582 disorders: a review. *Taiwanese journal of obstetrics & gynecology* 51 (1):12-17.  
583 doi:10.1016/j.tjog.2012.01.004
- 584 21. Alkuraya FS, Cai X, Emery C, Mochida GH, Al-Dosari MS, Felie JM, Hill RS, Barry BJ,  
585 Partlow JN, Gascon GG, Kentab A, Jan M, Shaheen R, Feng Y, Walsh CA (2011) Human  
586 mutations in NDE1 cause extreme microcephaly with lissencephaly [corrected]. *Am J Hum*  
587 *Genet* 88 (5):536-547. doi:10.1016/j.ajhg.2011.04.003
- 588 22. Bakircioglu M, Carvalho OP, Khurshid M, Cox JJ, Tuysuz B, Barak T, Yilmaz S,  
589 Caglayan O, Dincer A, Nicholas AK, Quarrell O, Springell K, Karbani G, Malik S, Gannon  
590 C, Sheridan E, Crosier M, Lisgo SN, Lindsay S, Bilguvar K, Gergely F, Gunel M, Woods CG  
591 (2011) The essential role of centrosomal NDE1 in human cerebral cortex neurogenesis. *Am J*  
592 *Hum Genet* 88 (5):523-535. doi:10.1016/j.ajhg.2011.03.019
- 593 23. Hu WF, Pomp O, Ben-Omran T, Kodani A, Henke K, Mochida GH, Yu TW, Woodworth  
594 MB, Bonnard C, Raj GS, Tan TT, Hamamy H, Masri A, Shboul M, Al Saffar M, Partlow JN,  
595 Al-Dosari M, Alazami A, Alowain M, Alkuraya FS, Reiter JF, Harris MP, Reversade B,  
596 Walsh CA (2014) Katanin p80 regulates human cortical development by limiting centriole  
597 and cilia number. *Neuron* 84 (6):1240-1257. doi:10.1016/j.neuron.2014.12.017
- 598 24. Kumar RA, Pilz DT, Babatz TD, Cushion TD, Harvey K, Topf M, Yates L, Robb S,  
599 Uyanik G, Mancini GM, Rees MI, Harvey RJ, Dobyns WB (2010) TUBA1A mutations cause  
600 wide spectrum lissencephaly (smooth brain) and suggest that multiple neuronal migration  
601 pathways converge on alpha tubulins. *Human molecular genetics* 19 (14):2817-2827
- 602 25. Cushion TD, Dobyns WB, Mullins JG, Stoodley N, Chung SK, Fry AE, Hehr U, Gunny  
603 R, Aylsworth AS, Prabhakar P, Uyanik G, Rankin J, Rees MI, Pilz DT (2013) Overlapping  
604 cortical malformations and mutations in TUBB2B and TUBA1A. *Brain* 136 (Pt 2):536-548.  
605 doi:10.1093/brain/aws338
- 606 26. Bahi-Buisson N, Poirier K, Fourniol F, Saillour Y, Valence S, Lebrun N, Hully M, Bianco  
607 CF, Boddaert N, Elie C, Lascelles K, Souville I, Consortium LI-T, Beldjord C, Chelly J  
608 (2014) The wide spectrum of tubulinopathies: what are the key features for the diagnosis?  
609 *Brain* 137 (Pt 6):1676-1700. doi:10.1093/brain/awu082

- 610 27. Tian G, Jaglin XH, Keays DA, Francis F, Chelly J, Cowan NJ (2010) Disease-  
611 associated mutations in TUBA1A result in a spectrum of defects in the tubulin folding and  
612 heterodimer assembly pathway. *Human molecular genetics* 19 (18):3599-3613
- 613 28. Jaglin XH, Chelly J (2009) Tubulin-related cortical dysgeneses: microtubule dysfunction  
614 underlying neuronal migration defects. *Trends Genet* 25 (12):555-566
- 615 29. Poirier K, Saillour Y, Bahi-Buisson N, Jaglin XH, Fallet-Bianco C, Nabbout R,  
616 Castelnau-Ptakhine L, Roubertie A, Attie-Bitach T, Desguerre I, Genevieve D, Barnerias C,  
617 Keren B, Lebrun N, Boddaert N, Encha-Razavi F, Chelly J (2010) Mutations in the neuronal  
618  $\alpha$ -tubulin subunit TUBB3 result in malformation of cortical development and neuronal  
619 migration defects. *Human molecular genetics* 19 (22):4462-4473. doi:10.1093/hmg/ddq377
- 620 30. Saillour Y, Broix L, Bruel-Jungerman E, Lebrun N, Muraca G, Rucci J, Poirier K,  
621 Belvindrah R, Francis F, Chelly J (2013) Beta tubulin isoforms are not interchangeable for  
622 rescuing impaired radial migration due to *Tubb3* knockdown. *Human molecular genetics*.  
623 doi:10.1093/hmg/ddt538  
624  
625



ACCEPTED MANUSCRIPT



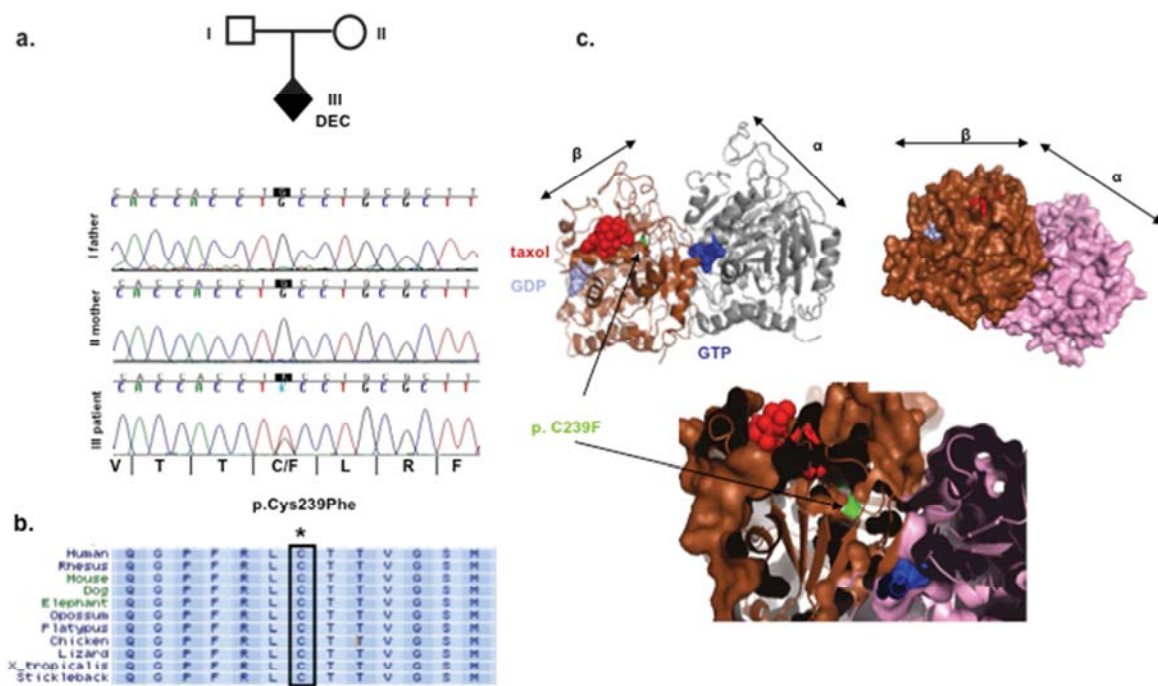
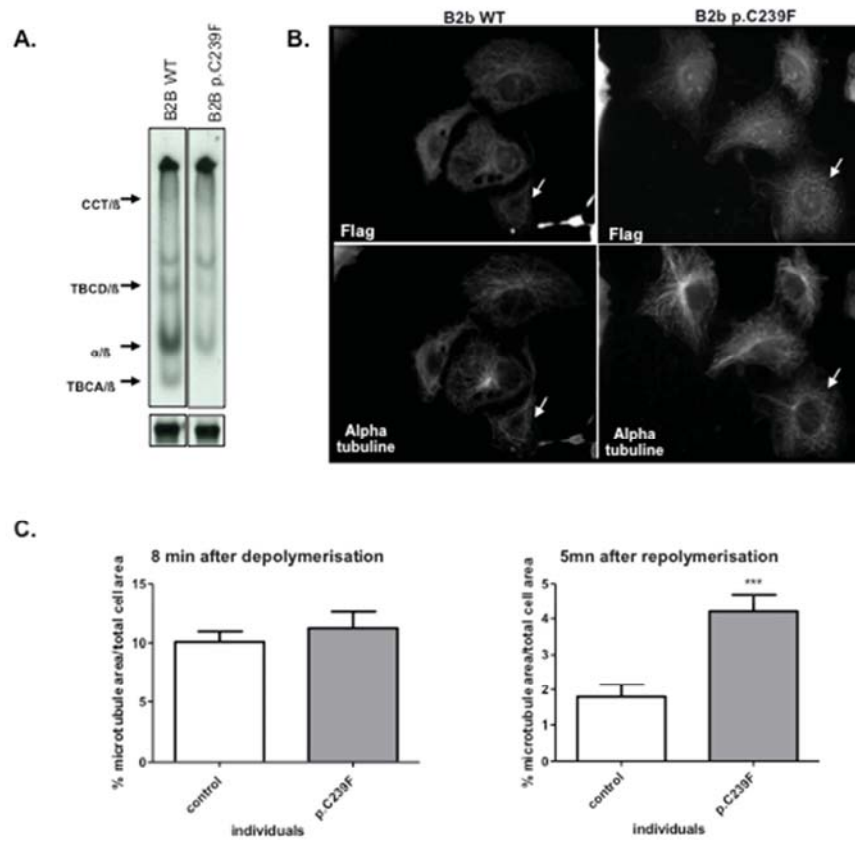
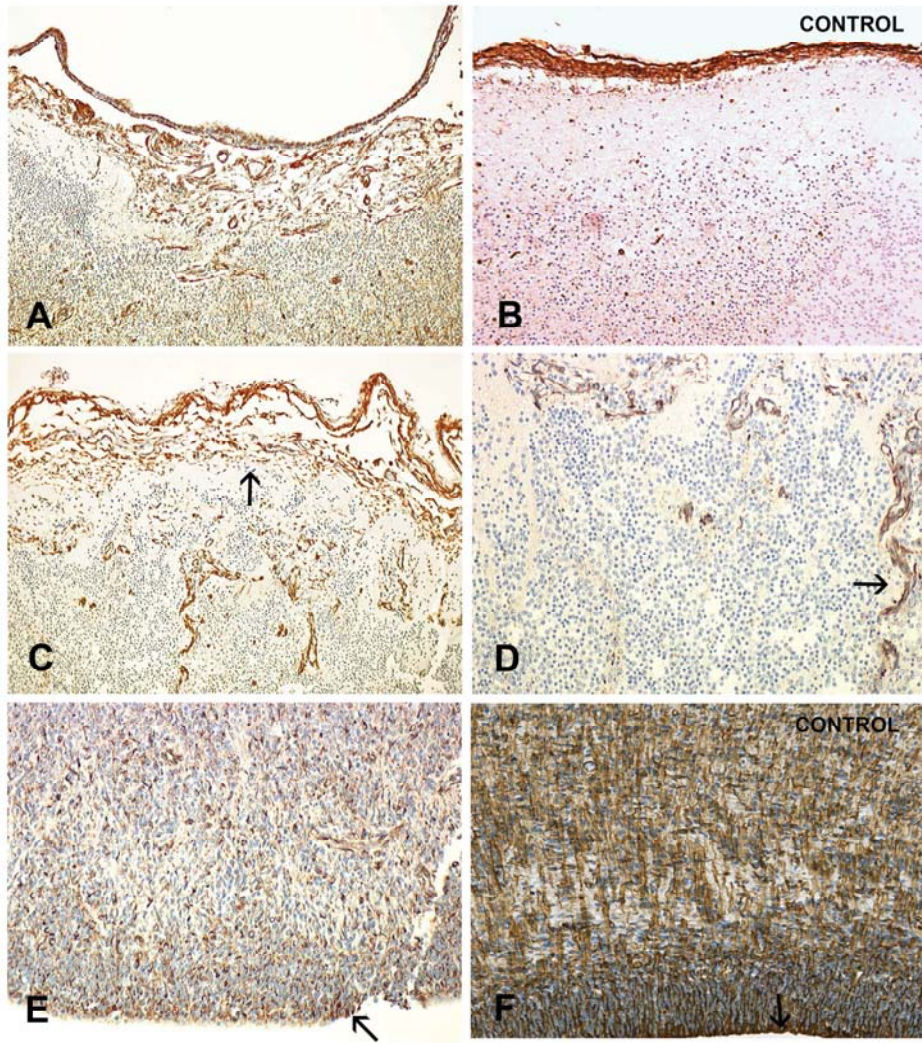


Figure 4





ACCEPTED